ISBN: 978-3-95450-231-8 ISSN: 2673-5490 doi: 10.18429/JACoW-IPAC2023-MOPL162

PARAMETER RANGES FOR A CHAIN OF RAPID CYCLING SYNCHROTRONS FOR A MUON COLLIDER COMPLEX*

A. Chancé† Université Paris-Saclay – CEA – Irfu, France
D. Amorim, F. Batsch, F. Boattini, L. Bottura, C. Carli, H. Damerau,
A. Grudiev, I. Karpov, E. Métral, D. Schulte, K. Skoufaris
CERN, Geneva, Switzerland

Abstract

A facility for a muon collider brings the big advantages of a compact lepton collider and a collision energy up to several TeV, well above the energy reach of conventional electron circular accelerators. However, the short lifetime of muons drives the design of the accelerator complex and collider, which makes this complex unique. A high muon survival rate and luminosity requires an extremely fast energy increase in combination with intense and ultra-short bunches. The International Muon Collider Collaboration proposes a chain of rapid cycling synchrotrons (RCS) for acceleration from several tens of GeV to several TeV. The minimization of the muon decay during the acceleration process is driven by technological limitations like the maximum magnet ramp and field, and cavity gradient. We will consider different scenarios to reuse as much as possible the existing infrastructure at CERN. We will give some scaling laws for a hybrid RCS to evaluate the frequency shift due to a path variation and the trajectory variation. Finally, we will propose a preliminary parameter range for the different stages of an RCS chain.

INTRODUCTION

A design proposal for a multi-TeV collision muon facility is developed in the framework of the International Muon Collider Collaboration (IMCC). The current baseline [1] facility, inspired by the US Muon Acceleration Program (MAP) [2, 3], produces one μ^+ and one μ^- bunch with a repetition rate of 5 Hz through proton irradiation of a target, cools them down, accelerates them to an energy of ≈ 60 GeV, injects and accelerates them in rapid cycling synchrotrons (RCS) up to the nominal energy, stores them in a ring for collisions at 10 TeV center-of-mass.

The Lorentz factor $\gamma(t)$ can be seen as a measure for the variation of the beam energy during the ramp. The survival rate of the muons $N_{\text{ext}}/N_{\text{inj}}$ is directly given for a general and linear ramp of duration, t_{ramp} by [4]:

$$\frac{N_{\text{ext}}}{N_{\text{inj}}} = e^{-\int_{t_{\text{inj}}}^{t_{\text{ext}}} \frac{dt}{\gamma(t)\tau_\mu}} \qquad \left.\frac{N_{\text{ext}}}{N_{\text{inj}}}\right|_{\text{linear}} = \left(\frac{\gamma_{\text{ext}}}{\gamma_{\text{inj}}}\right)^{\frac{t_{\text{ramp}}}{(\gamma_{\text{inj}}-\gamma_{\text{ext}})\tau_\mu}} \tag{1}$$

That implies that because of the short lifetime of the muons $\tau_\mu = 2.197\,\mu\text{s}$ in the rest frame and thanks to time dilatation, the order of magnitude of the total acceleration time in the RCS should be a few milliseconds to keep most of the muons.

Due to the considerable level of peak power required to rapidly ramp up the bending field, the current approach is to use resonant discharge circuits. Studies have shown that dual harmonics discharge circuits can provide close to linear B_{ref} shapes during the acceleration [5, 6]. However, a pure linear acceleration profile will probably be extremely expensive because of the huge correcting power that the converter electronics would have to provide via an active filter. Since the acceleration is very fast, the compensation of a non-linear ramp is made by modulating the synchronous phase in the cavities.

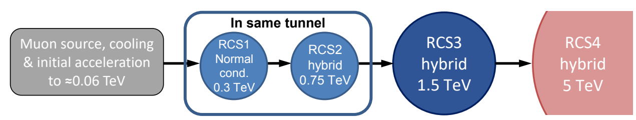

Figure 1: Schematic of the chain of RCSs for the high-energy acceleration complex.

Figure 1 shows a sketch of the high-energy acceleration stage. The two first RCS share the same tunnel and layout. Contrary to other RCS, the RCS1 uses only pulsed magnets. The other RCSs are hybrid ones. That means that pulsed magnets (generally normal conducting, NC) are interleaved with static magnets (generally superconducting, SC). The main motivation is to combine a rapid cycling (given by the pulsed dipoles) with a small circumference (given by the strong static dipoles). The possibility to reuse the LHC tunnel to host a fourth RCS is under discussion. This fourth RCS would later accelerate the muon bunches from 1.5 TeV to 4.2 TeV for the 8.4 TeV collider. Reaching an energy of 5 TeV may require a fifth RCS in the LHC tunnel or a larger circumference for the intermediate RCS.

We focus here on the chain of the four RCS to reach the collision energy. After giving some scaling laws for a hybrid RCS, we will scan the magnet fields to show the sensitivity of the acceleration scheme.

SCALING LAWS FOR A HYBRID RCS

If we assume that the magnetic rigidity is $B\rho_{\text{inj}}/B\rho_{\text{ext}}$ at injection/extraction and that the field is respectively $-B_{\text{NC}}/+B_{\text{NC}}$ at injection/extraction in the pulsed NC magnet and B_{SC} in the SC static dipole, we get the relationships for the total

* This work was supported by the European Union grant agreement 101094300.
† antoine.chance@cea.fr

ISBN: 978-3-95450-231-8 ISSN: 2673-5490 doi: 10.18429/JACoW-IPAC2023-MOPL162

length of the NC/SC dipoles $L_{\mathrm{T,\,NC}}$ and $L_{\mathrm{T,\,SC}}$ [3,7]:

$$L_{\mathrm{T,\,NC}} = \pi\frac{B\rho_{\mathrm{ext}} - B\rho_{\mathrm{inj}}}{B_{\mathrm{NC}}}; \quad L_{\mathrm{T,\,SC}} = \pi\frac{B\rho_{\mathrm{ext}} + B\rho_{\mathrm{inj}}}{B_{\mathrm{SC}}} \quad (2)$$

During the acceleration, the curvature radius is different in the two dipole families, which implies a trajectory variation as shown in Fig. 2. The question here is to evaluate the path length variation during the ramp, and also the distance between the different orbits to constrain the minimum dipole aperture.

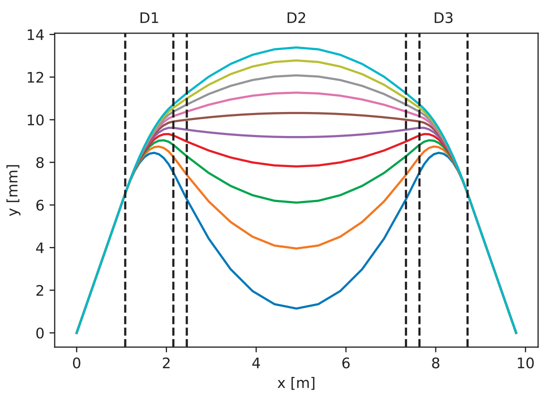

Figure 2: Trajectories in a half-cell for RCS2 with the parameters given in Table 1. The injection/extraction orbits are respectively in the inner/outer side (in blue/cyan).

Let $\mathscr{C}$ be the total length of the ring, L_{arc} the total length of the arcs made of n_c cells. We assume that $n_c \gg 1$. The length L_c and bending angle θ_c of an arc cell are thus:

$$L_c = \frac{L_{\mathrm{arc}}}{n_c} \qquad \theta_c = \frac{2\pi}{n_c} \ll 1 \qquad (3)$$

We will consider here two dipole families in the arc although the scaling laws have been generalized to an arbitrary number of families. We will respectively use the subscripts 1 and 2 for the dipole families and note D_1 and D_2 the two dipoles. The dipole sequence is done by alternating the two families: $D_1 - D_2 - \ldots - D_2 - D_1$. Each half-cell has thus $n_d + 1$ dipoles D_1 and n_d dipoles D_2. The total number of dipoles per cell is thus: $2 \times (2n_d + 1)$. We will assume that all dipoles are straight with parallel edges in a half-cell. Let be:

L_{dd}	distance between 2 dipoles
L_i	straight length of D_i
$L_{T,1} = 2n_c(n_d + 1)L_1$	total length of D_1
$L_{T,2} = 2n_c n_d L_2$	total length of D_2
$L_T = L_{T,1} + L_{T,2}$	total length of dipoles
$h^* = 1/\rho^*$	reference curvature
$h_i = 1/\rho_i$	bending curvature of D_i
$\mathscr{S}_T$	total path length
$\mathscr{S}^*_{T,a}$	total path length if $b = 1$

Let the following parameters describe the arc cell:

$$a = \frac{L_{T,2}}{L_T} \qquad b = \frac{h_2}{h^*} \qquad e_0 = \sin\frac{\pi}{2n_c} \qquad (4)$$

After some geometry, we get the following relationships for the dipoles D_1 and D_2:

$$h^* = \frac{4n_c}{L_T}e_0 \qquad h_1L_1 + h_2L_2 = \frac{2\,(ab + n_d)}{n_d(1 + n_d)}e_0 \qquad (5)$$

$$h_1 = \frac{1 - ab}{1 - a}h^* \qquad L_1 = \frac{1 - a}{2n_c(n_d + 1)}L_T \qquad (6)$$

$$h_2 = b \cdot h^* \qquad L_2 = \frac{a}{2n_c n_d}L_T \qquad (7)$$

It is worth noting the particular values for the set (a, b):

- $b = 1$: iso-magnetic case. We get: $h_1 = h_2 = h^*$.
- $b = 0$: the dipole D_2 is a drift.
- $b = 1/a$: the dipole D_1 is a drift.
- $a = 0$: the length of D_2 is 0.
- $a = 1$: the length of D_1 is 0. To avoid some singularity on the dipole field in D_1, we have to use $b = 1$ at the same time.

The variation on the total path length becomes:

$$\mathscr{S}_T - \mathscr{S}^*_{T,a} = \frac{a(b-1)\pi^2}{3n_d(1 + n_d)n_c}\Bigg[L_T\frac{ab + n_d}{4n_c} + L_{dd}\left(n_d(n_d - 1) + a(b + 1)(1 + 2n_d)\right)\Bigg] + o\left(\frac{1}{n_c^2}\right) \quad (8)$$

For $n_c \gg 1$, the maximum trajectory difference between the injection and extraction in the middle dipole is given by:

$$\Delta y_{\mathrm{mid}} \approx -\frac{\pi a \Delta b}{16n_c^2}\begin{cases}\dfrac{L_T + 4n_cL_{dd}n_d}{1 + n_d} & \text{if } n_d \text{ even}\\[2mm] \dfrac{L_T + 4n_cL_{dd}(1 + n_d)}{n_d} & \text{if } n_d \text{ odd}\end{cases} \quad (9)$$

We assume that the phase advance per arc FODO cell is 90°, the momentum compaction of the RCS is:

$$\alpha = \left(\frac{\pi}{n_c}\right)^2\Bigg\{\frac{1}{\sin^2\frac{\mu}{2}} - \frac{1}{4} + \frac{L_T}{6L_{\mathrm{arc}}} + \frac{ab + n_d}{6L_{\mathrm{arc}}n_d(1 + n_d)}\Big[a(1 - b)L_T + 4n_c(n_d(2 + n_d) - ab(1 + 2n_d))L_{dd}\Big]\Bigg\} \quad (10)$$

We see that for very large n_c, the path length, and trajectory difference scale as L_{dd}/n_c. For intermediate n_c (when the filling factor stays large enough to neglect the total distance between dipoles in comparison with the total dipole length), the total path length, and trajectory difference scale as L_T/n_c^2. The momentum compaction is proportional to $1/n_c^2$. In the particular case of $ab = -n_d$, we see that the path length difference only depends on the distance between the dipoles.

PARAMETER SCAN

The longitudinal dynamics shows that the large synchrotron tune asks for distributed RF stations [8]. To keep the longitudinal emittance increase below 5%, it is necessary to have at least 32 RF stations for RCS1, and 24 stations for the others. To keep some space for injection and extraction in the RCS, the corresponding number of arcs is 34 for

ISBN: 978-3-95450-231-8 ISSN: 2673-5490 doi: 10.18429/JACoW-IPAC2023-MOPL162

RCS1 and 26 for the others. We have kept a supersymmetry of the RCS and assumed the same number of cells per arc. Equation (2) gives the total length of the NC and SC dipoles. However, the parameters a and b defined in Eq. (4) depend on the order of the NC and SC dipoles. That is why we consider both cases. Figure 3 shows the variation of the path length and orbit difference in RCS2 versus the field in the SC dipoles, for different numbers of dipoles per half-cell and if the dipole pattern begins with a NC or SC dipole. The number of cells has been optimized to maximize the filling factor of the arcs by keeping enough space for the RF cavities. The variation is stepwise because of the supersymmetry.

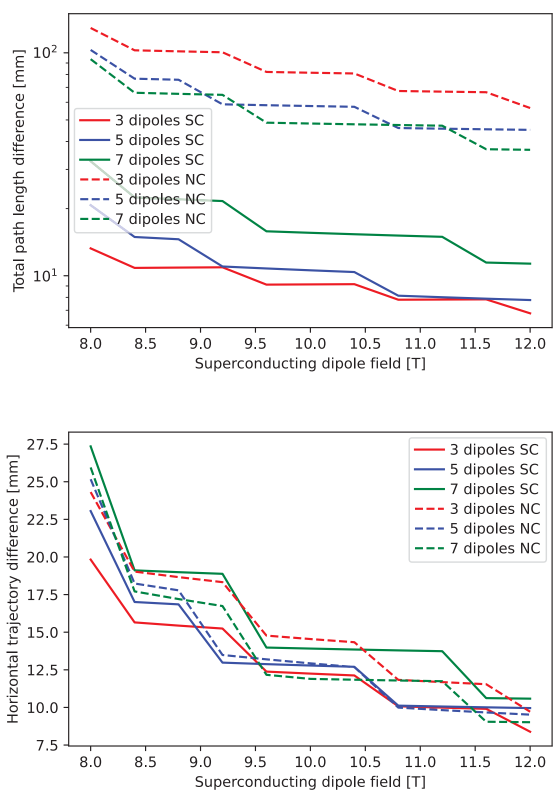

Figure 3: Path length (top) and orbit difference (bottom) as function of the SC dipole field in RCS2 with the other parameters given in Table 1. The dashed/solid lines are in the case with the NC/SC dipole first in the half-cell. The red/blue/green lines are in the case of 3/5/7 dipoles per half-cell. The number of cells n_c is optimized to maximize the filling ratio of the arcs.

The study shows that putting the SC dipole first allows to significantly reduce the total path length difference. In the study, only one pattern is inserted between two quadrupoles. A solution to reduce the total path length difference can be also to insert two magnet sets between two quadrupoles. However, because of the small number of cells per arc, that can be of interest only for RCS3 or RCS4. The orbit variation in the dipoles can be as large as 13 mm, which implies a minimum width of 19.6 mm for RCS2. The minimum width of the magnets only integrates the needs due to the beam size and orbit difference; it does not take into account the limitations coming from collective effects or magnet shieldings. The shielding requirements will significantly increase the inner aperture of the dipoles and ask for a dedicated study.

Table 1: Example parameters for the muon RCSs for an RF system at 1.3 GHz. Parameters for RCS4 are preliminary. The momentum compaction α_p is indicative and assumes FODO cells with a phase advance of 90°.

	RCS1	**RCS2**	**RCS3**	**RCS4**
Hybrid RCS	No	Yes	Yes	Yes
Circumference [m]	5990	5990	10700	26659
Injection energy [TeV]	0.06	0.30	0.75	1.5
Extraction energy [TeV]	0.30	0.75	1.50	4.2
Survival rate [%]	90	90	90	90
Acceleration time [ms]	0.34	1.10	2.37	5.75
Number of turns	17	55	66	65
Energy gain/turn [GeV]	14.8	7.9	11.4	41.5
NC dipole field [T]	0.36/1.8	-1.8/1.8		
SC dipole field [T]	-	10	10	16
Number of arcs	34	26	26	26
Number of cells/arc	7	10	17	19
NC dipoles/half cell, n_d	1	1	1	2
Cell length [m]	21.4	19.6	20.6	45.9
NC dipole length [m]	2.6	4.9	4.9	8.0
SC dipole length [m]	-	1.1	1.3	1.3
Dipole spacing, L_{dd} [mm]	0.3			
Quadrupole length [m]	2			
Norm. emittance [μm]	25			
α_p [10^{-4}]	3.3	2.4	0.89	0.72
Path length diff. [mm]	0	9.1	2.7	9.4
Orbit difference [mm]	0	12.2	5.9	13.2
Beam stay clear [σ]	6			
Min. dipole width [mm]	17.4	19.6	10.7	18.8
Min. dipole height [mm]	14.8	6.4	4.2	4.4

CONCLUSION

We presented the scaling laws for a hybrid synchrotron with two dipole families. We have then applied them to the RCS chain for muon acceleration. In the case of FODO cells in the arcs, the study shows that a pattern of three dipoles with the SC dipole in the middle enables to keep a variation of the path length below one centimetre in the second RCS. The optimisation includes the constraint of at least 24 distributed RF stations. We give also the orbit differences from injection to extraction for the hybrid RCS and thus a minimum aperture for the magnets.

REFERENCES

[1] D. Schulte, *et al.*,“Bright Muon Beams and Muon Colliders”, in European Strategy for Particle Physics - Accelerator R&D Roadmap, CERN-2022-001, p. 145, 2022. doi:10.23731/CYRM-2022-001

ISBN: 978-3-95450-231-8 ISSN: 2673-5490 doi: 10.18429/JACoW-IPAC2023-MOPL162

[2] M. A. Palmer, "Muon Accelerator Program (MAP)". http://map.fnal.gov

[3] J. S. Berg, "Details and justifications for the MAP concept specification for acceleration above 63 GeV", BNL-105415-2014-IR, 2014. doi:10.2172/1149436

[4] T. Dascalau, *et al.*, "A Design for a 3 TeV Rapid Cycling Synchrotron for Muon Acceleration in the SPS Tunnel", CERN report, 2020. doi:10.17181/CERN.YA66.G3H6

[5] F. Boattini, "Powering solutions and technology", presented at IMCC Annual Meeting 2022, CERN, Switzerland, 11-14 October 2022.

[6] F. Boattini, D. Aguglia, L. Bottura, and G. Brauchli, "A two harmonics circuit for the powering of the very fast RCS (Rapid Cycling Synchrotron) of the muon collider accelerator", presented at the IPAC'23, Venice, Italy, May 2023, paper WEPM078, this conference.

[7] J. S. Berg, "Muon Collider Pulsed Synchrotron Parameters", BNL-221336-2021-INRE, 2021. doi:10.2172/1779395

[8] F. Batsch *et al.*, "Longitudinal Beam Dynamics and RF Requirements for a Chain of Muon RCSs", presented at the IPAC'23, Venice, Italy, May 2023, paper TUPA040, this conference.